MOLECULAR AND CELLULAR BIOLOGY, July 2004, p. 5887–5899 Vol. 24, No. 13
0270-7306/04/$08.00+0 DOI: 10.1128/MCB.24.13.5887–5899.2004

Targeted Inactivation of Testicular Nuclear Orphan Receptor 4 Delays and Disrupts Late Meiotic Prophase and Subsequent Meiotic Divisions of Spermatogenesis

Xiaomin Mu, Yi-Fen Lee, Ning-Chun Liu, Yei-Tsung Chen, Eungseok Kim, Chih-Rong Shyr, and Chawnshang Chang*

Departments of Pathology, Urology, and Radiation Oncology and Cancer Center, University of Rochester Medical Center, Rochester, New York 14642

Received 16 December 2003 /Returned for modification 8 January 2004 /Accepted 3 April 2004

Testicular orphan nuclear receptor 4 (TR4) is specifically and stage-dependently expressed in late-stage pachytene spermatocytes and round spermatids. In the developing mouse testis, the highest expression of TR4 can be detected at postnatal days 16 to 21 when the first wave of spermatogenesis progresses to late meiotic prophase. Using a knockout strategy to delete TR4 in mice, we found that sperm production in TR4$^{-/-}$ mice is reduced. The comparison of testes from developing TR4$^{+/+}$ and TR4$^{-/-}$ mice shows that spermatogenesis in TR4$^{-/-}$ mice is delayed. Analysis of the first wave of spermatogenesis shows that the delay can be due to delay and disruption of spermatogenesis at the end of late meiotic prophase and subsequent meiotic divisions. Seminiferous tubule staging shows that stages X to XII, where late meiotic prophase and meiotic divisions take place, are delayed and disrupted in TR4$^{-/-}$ mice. Histological examination of testis sections from TR4$^{-/-}$ mice shows degenerated primary spermatocytes and some necrotic tubules. Testis-specific gene analyses show that the expression of sperm 1 and cyclin A1, which are genes expressed at the end of meiotic prophase, was delayed and decreased in TR4$^{-/-}$ mouse testes. Taken together, results from TR4$^{+/+}$ and TR4$^{-/-}$ mice indicate that TR4 is essential for normal spermatogenesis in mice.

The orphan receptors belong to the nuclear receptor superfamily, members of which mediate extracellular signals to transcriptional response. The roles of orphan receptors have been linked to animal development, cellular differentiation, and homeostasis. The human testicular orphan receptor 4 (TR4) was originally isolated from testis and prostate cDNA libraries by PCR (3). While TR4 shares the structural features of nuclear receptors, no ligand has been identified, and it is therefore considered an orphan receptor. TR4 is relatively highly expressed in several tissues including testis, kidney, and muscle (6). Northern blot analyses from multiple human and mouse tissues show a 9.4- and a 2.8-kb transcript. The 9.4-kb transcript is expressed ubiquitously, while the 2.8-kb transcript is largely restricted to the testis (6, 7). In testes, TR4 is specifically expressed in germ cells (6, 7).

TR4 can modulate its target gene expression by forming homodimers and binding to AGGTCA direct repeat sequences in its target genes (9). We have demonstrated that TR4 can modulate many signal transduction pathways, such as those involving retinoic acid (11), the thyroid hormone (12), vitamin D (12), and ciliary neurotrophic factor (25). TR4 also can modulate transactivation mediated by other steroid nuclear receptors through interaction with these steroid receptors. Our group demonstrated that TR4 could interact with the androgen receptor (AR) and the estrogen receptor and thus suppress AR- and estrogen receptor-mediated transactivation (10, 19). Recently TR2 and TR4 heterodimers have been found in the core of a larger erythroid epsilon-globulin gene repressor complex called DRED, which represses embryonic and fetal globulin transcription in definitive erythroid cells (22).

Although TR4 is highly and specifically expressed in testes, its physiological functions remain unclear. Here we report some of the physiological functions of TR4 in spermatogenesis via studies of TR4-knockout (TR4$^{-/-}$) mice. Our results show that TR4 plays a critical role in the late meiotic prophase and subsequent divisions in mouse spermatogenesis.

MATERIALS AND METHODS

Genotyping of TR4$^{-/-}$ mice. Mice used in these studies were genotyped from tail biopsy specimen DNA via PCR analyses. The primers used for wild-type allele amplification were 5′-GGAGACACACTGCAGATGTCCGAATAC-3′ (A) and 5′-CACAGCTCATTTCTCTGCTCACTTACTC-3′ (B), which are located between exons 4 and 5 of the TR4 gene. The primers used to amplify the mutant allele were 5′-TGCAAGCATACTTCTTGTTCC-3′ (C) and 5′-GCAG CGCATCGCCTTCTATC-3′ (D). Primer C is located in the Neo sequence of the LacZ/MCI-Neo selection cassette, and primer D is located between exons 5 and 6 of the TR4 gene.

Histological analysis. Tissues were fixed in fresh 10% neutral buffered formalin, Bouin's fixative, or Forman-Zender buffer and embedded in paraffin. Tissue sections were stained with hematoxylin, eosin, or periodic acid and Schiff reagent (PAS) and examined by light microscopy.

RT and real-time quantitative RT-PCR. Mouse testes from TR4$^{+/+}$ and TR4$^{-/-}$ mice at various ages were dissected, and total RNA was isolated using Trizol reagent (Invitrogen). cDNA synthesis and PCR were performed using SuperScript II RNase H$^-$ reverse transcriptase and the cDNA cycle kit (Invitrogen) according to the manufacturer's protocol. Real-time quantitative reverse transcription-PCR (RT-PCR) was performed using the iCycler real-time PCR amplifier (Bio-Rad Laboratories) as described previously (14). Each PCR was performed in triplicate, and each experiment was repeated twice. The results were normalized with β-actin. Real-time quantitative PCR results were calculated after adjusting for actin using $2^{-\Delta Ct}$, where ΔCt equals target gene Ct − actin Ct. A list of the primer sequences for RT-PCR and real-time quantitative PCR is available upon request.

* Corresponding author. Mailing address: Departments of Pathology, Urology, and Radiation Oncology and Cancer Center, University of Rochester Medical Center, Rochester, NY 14642. Phone: (585) 273-4500. Fax: (585) 756-4133. E-mail: chang@urmc.rochester.edu.

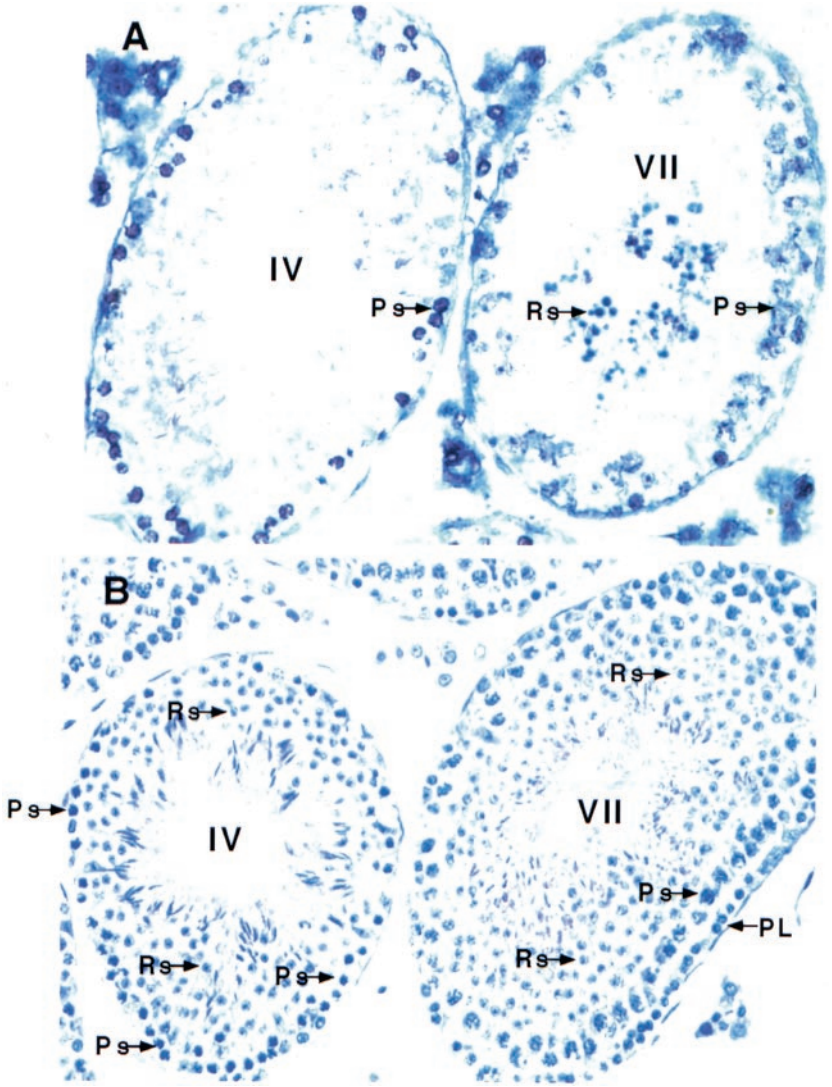

FIG. 1. TR4 is cell-specifically expressed in pachytene spermatocytes and stage-dependently expressed in round spermatids. (A) In situ hybridization of normal adult testis sections with antisense TR4 digoxigenin-labeled probe. Seminiferous tubules in stages IV and VII, which show positive signals in pachytene spermatocytes and in both pachytene spermatocytes and spermatids, respectively, are shown. (B) PAS and hematoxylin staining of two seminiferous tubules in panel A, in a consecutively cut section. Sections from three $TR4^{+/+}$ and $TR4^{-/-}$ mice were examined. A representative slide is shown in each panel. Ps, pachytene spermatocytes; Rs, round spermatids; PL, prelepotene spermatocytes. Magnification, ×400.

In situ hybridization. Digoxigenin-UTP-labeled riboprobes were prepared with the DIG RNA labeling kit (Roche Molecular Biochemicals) from linearized plasmid DNA templates. Tissues were fixed and embedded in paraffin, and 5-μm sections were cut and mounted on coated slides. Tissues on slides were dehydrated, postfixed, and acetylated as described previously (15). After hybridization, slides were washed and exposed to alkaline phosphatase-conjugated anti-digoxigenin antibody, and riboprobes were detected with nitroblue tetrazolium chloride and 5-bromo-4-chloro-3-indolylphosphate (BCIP)–4-toluidine substrate.

Southern blot analyses. Mouse genomic DNAs used in these studies were isolated from testis, digested with EcoRI, separated by electrophoresis through an 0.8% agarose gel, and transferred to a positively charged nylon membrane. A TR4 N-terminal probe was labeled with a random primer labeling kit (Amersham) and used in hybridizations. $TR4^{+/+}$ and $TR4^{-/-}$ mice were identified by predicted restriction fragment size differences.

Detection and characterization of apoptotic germ cells. We used the terminal deoxynucleotidyltransferase-mediated dUTP-biotin nick end labeling (TUNEL) assay to detect apoptosis using the Fluorescein-Frag EL DNA fragmentation detection kit (Oncogen; QIA 39) according to the manufacturer's protocol.

Sperm count. Caudae epididymides were removed from adult males and placed in a dish containing 5 ml of Dulbecco modified Eagle medium with 10% fetal calf serum. Sperm was allowed to disperse into medium for 1 h at 37°C, and numbers were counted with a hemacytometer under phase-contrast microscopy.

DNA flow cytometry analysis of testis cells. Ethanol-fixed testis cells (1×10^6 to 2×10^6) were treated with RNase (1 mg/ml) for 30 min at room temperature. After centrifugation, cells were stained with propidium iodide (PI; 40 μg/ml). The PI-stained cells were analyzed by flow cytometry (Epics Elite ESP; Coulter).

RESULTS

Cell-specific and stage-dependent expression of TR4. Since previous results indicated that TR4 was mainly expressed in germ cells, we further investigated the detailed expression of TR4 during spermatogenesis. In situ hybridization with a digoxigenin-labeled antisense TR4 cRNA probe, staining with PAS, and hematoxylin staining with the use of consecutive sections from $TR4^{+/+}$ mice show that TR4 is highly expressed

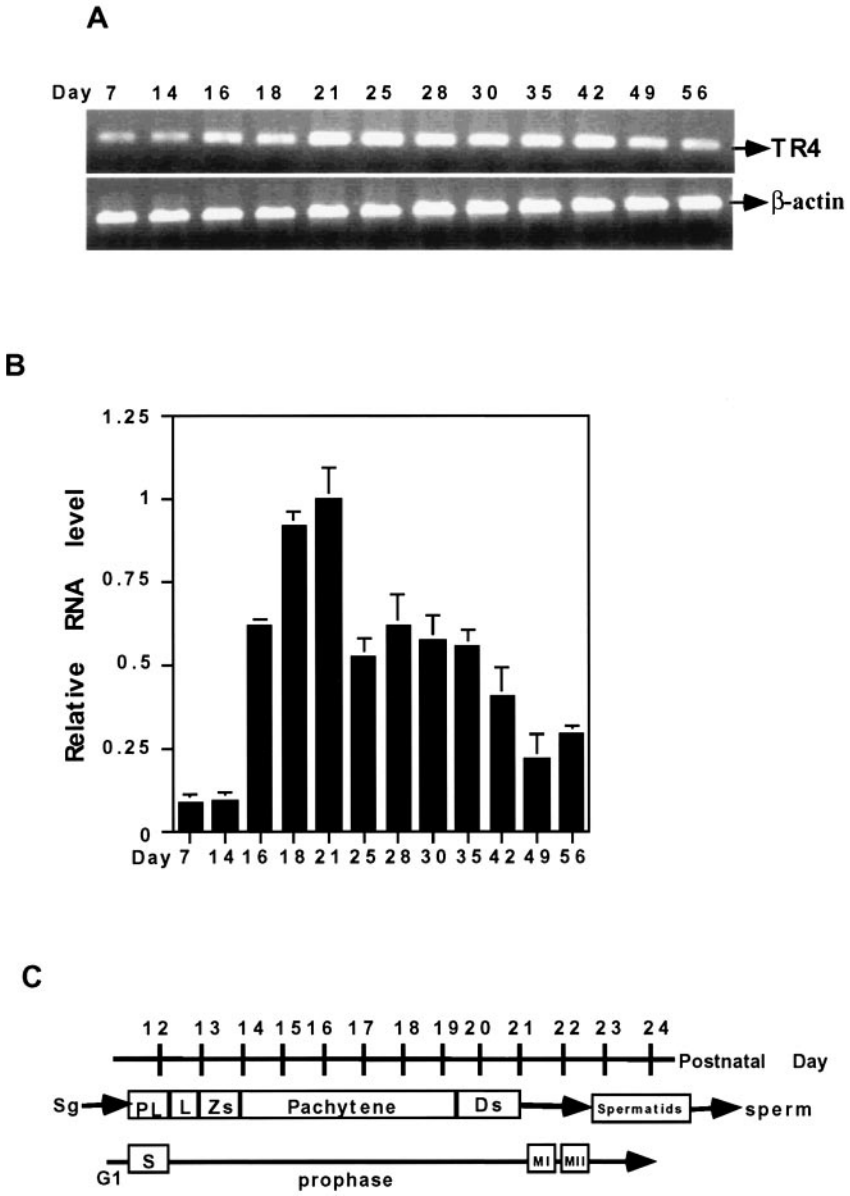

FIG. 2. Time course of TR4 expression during testis development. (A) Total RNA was isolated from testes of mice at different postnatal days as indicated. RT-PCR was performed, with β-actin as an internal control. (B) Total RNA was isolated from testes of mice at different postnatal days as indicated, and real-time quantitative RT-PCR was performed. Results are means ± standard deviations from two or three RNA samples from two or three different mice. All sets of results show the same trend, and one set of data is shown. (C) Timetable of first wave of spermatogenesis, including spermatogonia (Sg), the prelepotene (PL), lepotene (L), zygotene (Zs), pachytene, and diplotene (Ds) stages of germ cell differentiation.

in primary spermatocytes, especially in late-stage pachytene spermatocytes (Fig. 1). TR4 is also expressed in round spermatids. The expression of TR4 in round spermatids is stage dependent and can be detected only in stage VII (Fig. 1). We detected no specific hybridization when an antisense TR4 cRNA probe was replaced with the sense TR4 cRNA probe (data not shown).

Time course of TR4 expression during testis development. To define the stage where TR4 plays a role, we investigated the TR4 expression starting from testicular development continuing into adult stages. Total RNAs of $TR4^{+/+}$ mice of different ages were prepared and analyzed by RT-PCR (Fig. 2A) and real-time quantitative PCR (Fig. 2B). As shown in Fig. 2, expression of TR4 mRNA can be detected 1 week after birth, begins to increase at postnatal day 16, and reaches the highest level at around day 21. At day 25, TR4 expression begins to decrease and remains at a moderate level throughout the adult stage. Early studies (2) indicated that, between days 16 and 21, the first wave of spermatogenesis progresses at the meiotic prophase (Fig. 2C). TR4 expression in the developing testis (Fig. 2) is consistent with the results in Fig. 1, showing that TR4 is highly expressed in advanced pachytene spermatocytes, and suggests that TR4 plays significant roles in the late meiotic prophase and subsequent meiotic divisions.

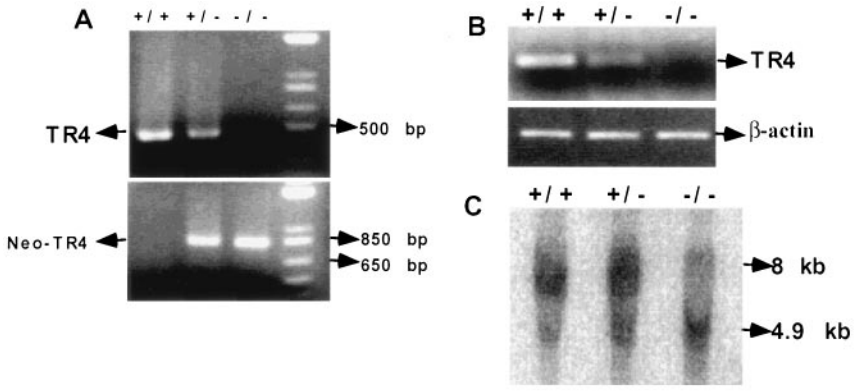

FIG. 3. Confirmation of knockout of TR4 gene in $TR4^{-/-}$ mice. (A) PCR analysis of mouse genomic DNA. The wild-type and target alleles give 455- and 760-bp PCR products, respectively. (B) RT-PCR analysis of TR4 in $TR4^{+/+}$, $TR4^{+/-}$, and $TR4^{-/-}$ mouse testes. Total RNAs from $TR4^{+/+}$, $TR4^{+/-}$, and $TR4^{-/-}$ mice were extracted, and RT-PCR was performed. (C) Southern blot analyses of mouse testis DNA from $TR4^{+/+}$, $TR4^{+/-}$, and $TR4^{-/-}$ mice. DNA was digested with EcoRI and hybridized with the probe indicated. The expected fragments after EcoRI digestion are 8 kb for the wild-type allele and 4.9 kb for the mutant allele.

Confirmation of knockout of the TR4 gene in $TR4^{-/-}$ mice. Using classic knockout and homologous recombination techniques, we were able to replace most of exon 4 and the complete exon 5 of the TR4 gene with the LacZ/MCI-Neo cassette to generate $TR4^{-/-}$ mice. (A complete description of generation and characterization of $TR4^{-/-}$ mice, with focus on the growth assays, behavior, and fertility studies related to $TR4^{-/-}$ mice, is in the manuscript submitted by L. L. Collins et al.) PCR analysis of DNA extracted from mouse tail biopsy specimens with two sets of primers, as described in Materials and Methods, shows that $TR4^{+/+}$ mice have an intact TR4 gene and $TR4^{-/-}$ mice have DNA deleted between exons 4 and 5 (Fig. 3A).

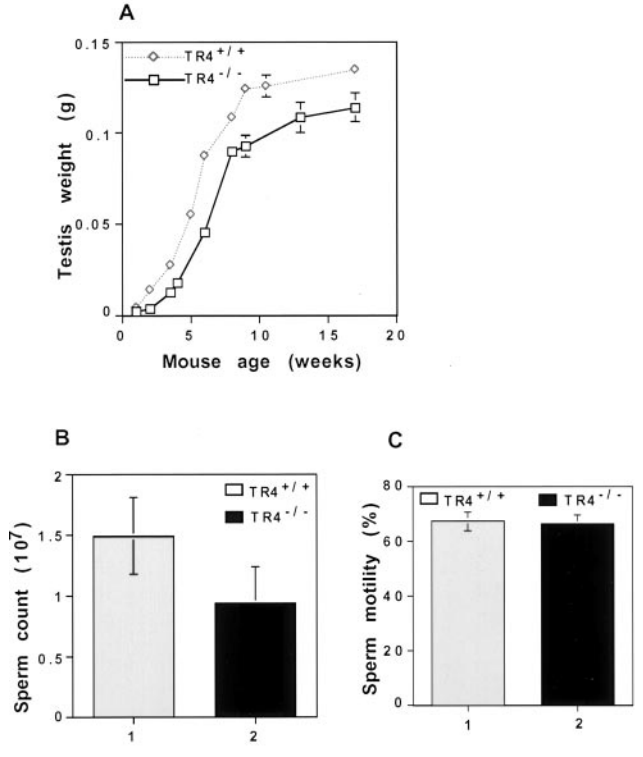

FIG. 4. Testis weight and sperm production in $TR4^{+/+}$ and $TR4^{-/-}$ mice. (A) Comparison of testis weights from $TR4^{+/+}$ and $TR4^{-/-}$ mice. Testes from $TR4^{+/+}$ mice and $TR4^{-/-}$ mice were removed, and the weights of testes were determined. At the different age points, two or three mice were used. (B and C) Comparison of sperm counts (B) and motility (C) from caudae epididymides between $TR4^{+/+}$ and $TR4^{-/-}$ mice. The sperm from caudae epididymides from more than five $TR4^{+/+}$ and $TR4^{-/-}$ mice, all at 2 to 3 months of age, were counted by hemacytometer under phase-contrast microscopy for total sperm (B) and sperm motility (C). Results are means ± standard deviations of at least five mice.

RT-PCR analyses of RNA extracted from the testes of 3-month-old $TR4^{+/+}$, $TR4^{+/-}$, and $TR4^{-/-}$ mice indicate that TR4 expression is decreased in $TR4^{+/-}$ mice and undetectable in $TR4^{-/-}$ mice (Fig. 3B). To further confirm the genotype of the $TR4^{-/-}$ mice in this study, we extracted genomic DNAs from the testes of $TR4^{+/+}$, $TR4^{+/-}$, and $TR4^{-/-}$ mice; digested them with EcoRI; and performed Southern blotting. As shown in Fig. 3C, Southern blotting demonstrated an 8-kb DNA fragment in $TR4^{+/+}$ mice, a 4.9-kb DNA fragment in $TR4^{-/-}$ mice, and both DNA fragments in $TR4^{+/-}$ mice as expected. Together, the results in Fig. 3 clearly demonstrated that the TR4 gene was successfully disrupted in $TR4^{-/-}$ mice.

Morphological appearance and weight of testis and sperm production in $TR4^{-/-}$ mice. $TR4^{-/-}$ mice are relatively smaller than $TR4^{+/+}$ mice. $TR4^{-/-}$ mice show varying degrees of behavioral defects, such as hypersensitivity to environmental stimulus, and breeding studies indicated that $TR4^{-/-}$ males had reduced fertility. To test fertility, we put five $TR4^{+/+}$ and five $TR4^{-/-}$ adult male mice together with seven $TR4^{+/+}$ adult females for 4 months. All of the $TR4^{+/+}$ males produced offspring. However, only one of the $TR4^{-/-}$ males produced offspring (Collins et al., submitted for publication). The sizes of adult $TR4^{+/+}$ and $TR4^{-/-}$ mouse testes are similar, but the weights of testes from $TR4^{-/-}$ mice at various developmental stages are lower than those of the $TR4^{+/+}$ mice (Fig. 4A). The sperm numbers are lower in $TR4^{-/-}$ mice at various ages than in $TR4^{+/+}$ mice. As shown in Fig. 4B, the cauda epididymis sperm numbers from 2- to 3-month-old $TR4^{-/-}$ mice are much lower than those of $TR4^{+/+}$ mice. However, there is no significant difference of cauda epididymis sperm mobility between $TR4^{+/+}$ and $TR4^{-/-}$ mice (Fig. 4C). We also examined sperm

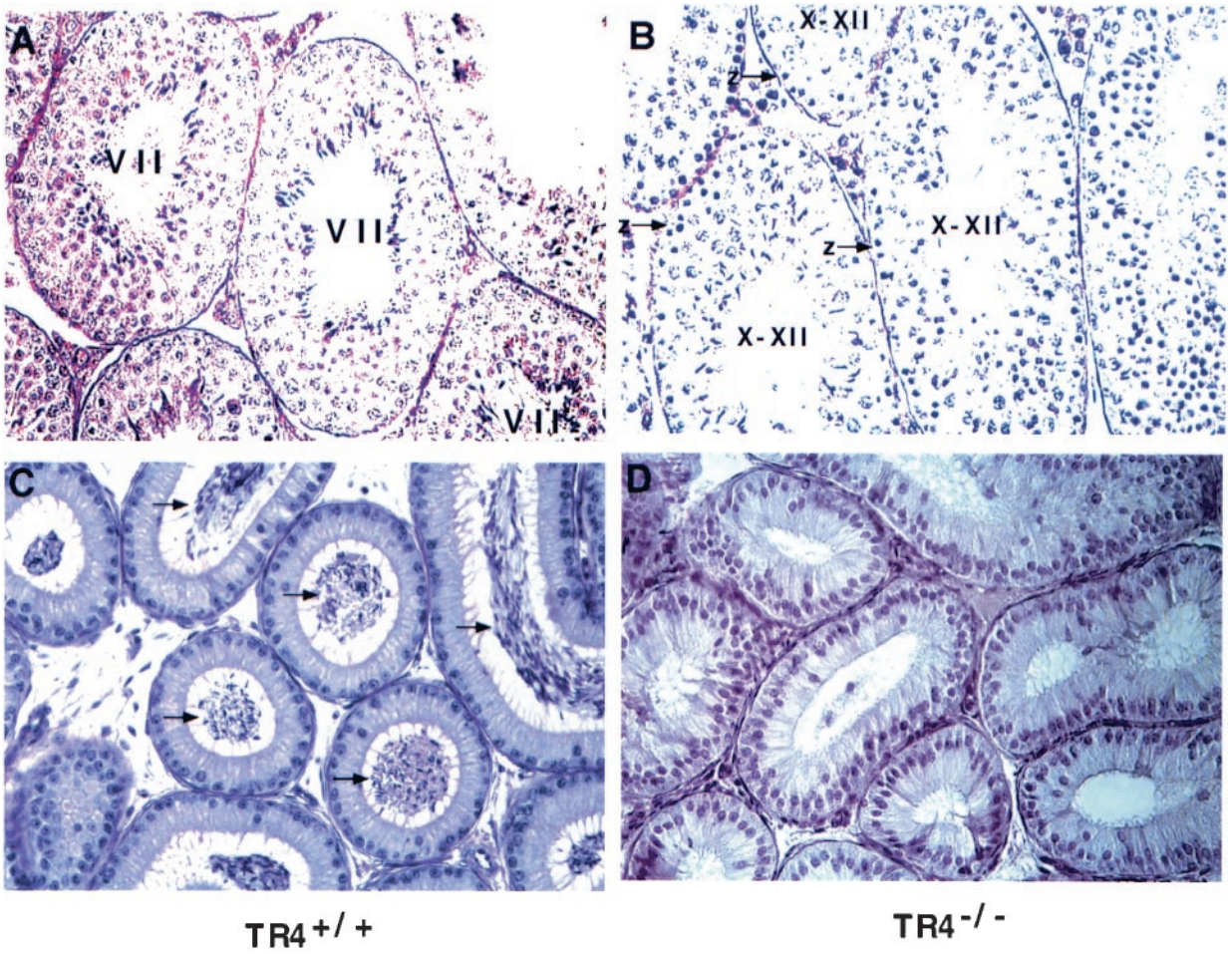

FIG. 5. Delayed spermatogenesis in TR4$^{-/-}$ mice. (A) PAS-hematoxylin staining of testes from 6-week-old TR4$^{+/+}$ mouse. Note that the stage VII seminiferous tubules were most frequently observed. (B) PAS-hematoxylin staining of testes from 6-week-old TR4$^{-/-}$ mouse. Note that testes lack stage VII seminiferous tubules and that the tubules at stages X to XII were most frequently observed. (C) Morphology of epididymides of TR4$^{+/+}$ mice at 6 weeks of age. Note that epididymides were full of sperm (arrows). (D) Morphology of epididymides from 6-week-old TR4$^{-/-}$ mice. Note that very few sperm can be seen in epididymides. Each panel shows a representative slide from examination of three TR4$^{-/-}$ or three TR4$^{+/+}$ mice. Magnification, ×400.

morphology by phase-contrast microscopy and found no significant differences between TR4$^{+/+}$ and TR4$^{-/-}$ mice. The lengths of cauda epididymis sperm flagella from TR4$^{+/+}$ and TR4$^{-/-}$ mice are similar, and the acrosome in the head of cauda epididymis sperm can be observed by PAS staining in both TR4$^{+/+}$ and TR4$^{-/-}$ mice.

Delayed spermatogenesis. Testis sections from 6-week-old TR4$^{+/+}$ mice usually show step 16 spermatids, and the most frequently seen tubules are stage VII. However, in 6-week-old TR4$^{-/-}$ mice, step 16 spermatids and typical stage VII tubules were seldom observed and the most frequently seen tubules were stage X to XII (Fig. 5, compare panel A with panel B). The typical stage VII tubules, however, started to be more frequently seen at about 10 weeks of age (data not shown). Furthermore, unlike 6-week-old TR4$^{+/+}$ mice with epididymides full of sperm, we observed some TR4$^{-/-}$ mice with few sperm in their epididymides (Fig. 5C versus D). These data suggest that the first wave of spermatogenesis in TR4$^{-/-}$ mice is delayed.

Delayed and disrupted late meiotic prophase and meiotic divisions of the first wave of spermatogenesis in juvenile TR4$^{-/-}$ mice. In order to unveil the mechanism of late spermatogenesis in TR4$^{-/-}$ mice, the progression of the first wave of spermatogenesis was compared in TR4$^{+/+}$ and TR4$^{-/-}$ littermates. At postnatal day 7, the testis histology results from both TR4$^{+/+}$ and TR4$^{-/-}$ mice are similar, spermatogenesis is arrested at spermatogonia stage, and seminiferous tubules contain Sertoli cells and spermatogonia (data not shown). As shown in Fig. 6, at day 14, when the premeiosis phase of spermatogenesis begins, germ cell differentiation in TR4$^{-/-}$ mice is nearly at the same stage or is only slightly slowed compared to that in the TR4$^{+/+}$ mice. At this stage germ cell differentiation proceeds to the stage of mostly zygotene spermatocytes (Fig. 6A versus B). At day 22 in TR4$^{+/+}$ mice some tubules have completed the first and second meiosis, many round spermatids can be seen in the tubules, and a few of them have differentiated into elongated spermatids (Fig. 6C). In some tubules, meiosis is in process and a few metaphase cells

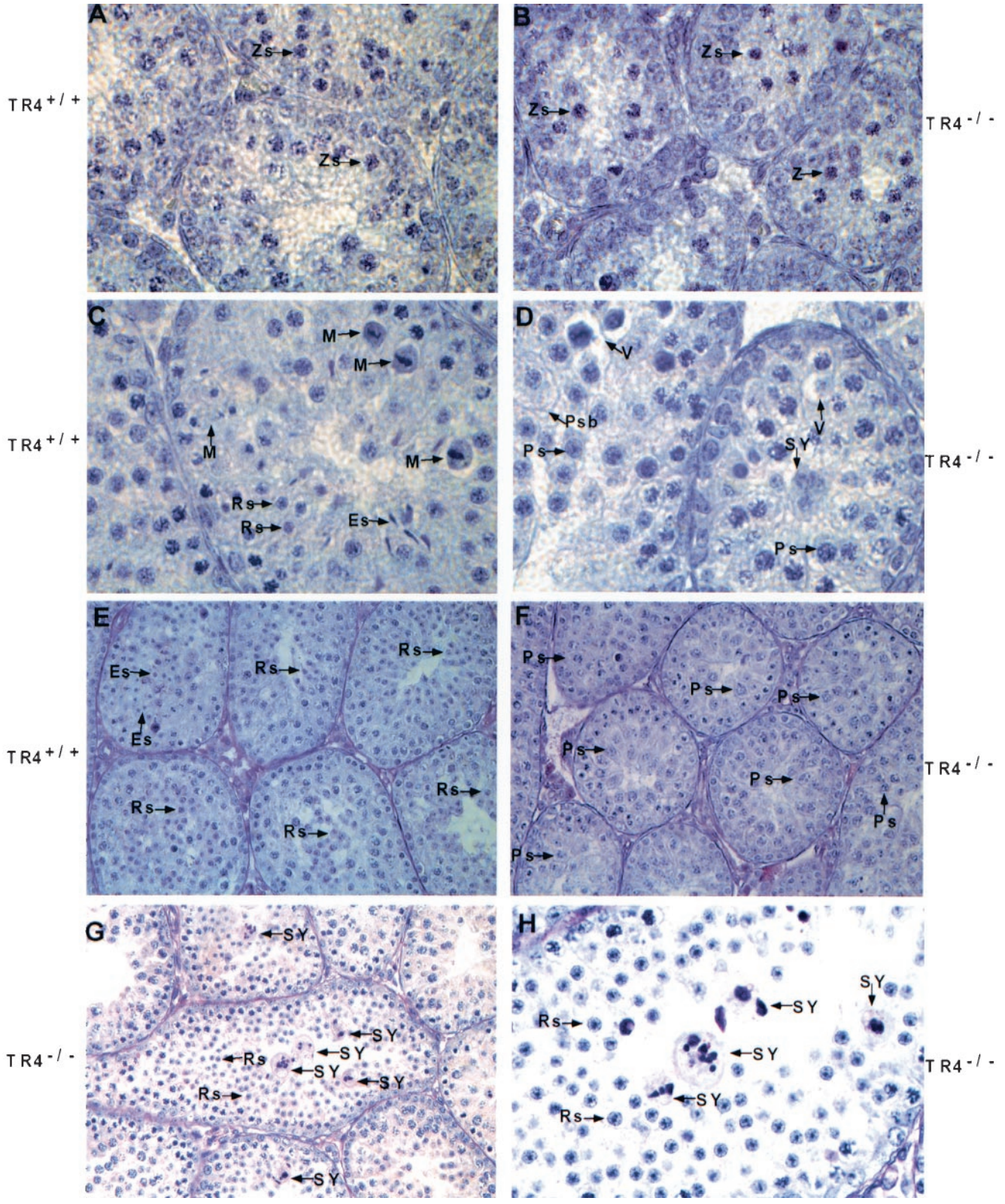

can be observed (Fig. 6C). However, in TR4$^{-/-}$ mice, at day 22, meiosis has not occurred, cells have arrested in meiotic prophase stage, and the most highly differentiated germ cells are still the late pachytene spermatocytes (Fig. 6D). Some pathological changes such as vacuoles in the cytosol of pachytene spermatocytes, multinucleated giant cells (i.e., symblasts [SY]), and primary spermatocytes with increased cytosol can be observed (Fig. 6D). At day 28, in TR4$^{+/+}$ mice, most

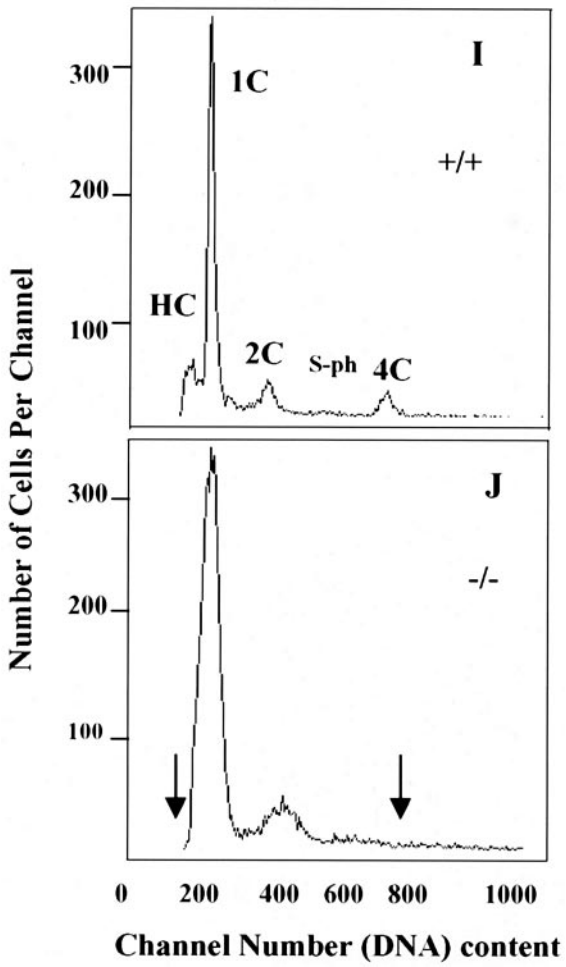

FIG. 6. Delayed and disrupted late meiotic prophase and subsequent meiotic divisions in first wave of spermatogenesis in $TR4^{-/-}$ mice. Morphology of seminiferous tubules from $TR4^{+/+}$ (A, C, and E) and $TR4^{-/-}$ (B, D, F, G, and H) mice at postnatal days 14 (A and B), 22 (C and D), 28 (E and F), and 31 (G and H) is shown. At day 14, germ cell differentiation progresses to mostly zygotene (Zs) stage in both $TR4^{+/+}$ and $TR4^{-/-}$ mice. At day 22, in $TR4^{+/+}$ mice, meiosis has been completed and many round spermatids (Rs) are produced, with a few of them being differentiated into elongated spermatids (Es). In $TR4^{-/-}$ mice cells were still arrested in pachytene (Ps) or diplotene stages, no round spermatids were produced, and tubules contained multinucleated giant cells (SY) and primary spermatocytes with increased cytosol (Psb). Vacuoles (V) in the cytosol of pachytene spermatocytes can be frequently observed. At day 28, adluminal cells are primarily round and elongated spermatids in $TR4^{+/+}$ mice, while adluminal cells are still primarily pachytene spermatocytes or diplotene spermatocytes in $TR4^{-/-}$ mice. At day 31, meiosis has been completed and round spermatids appear in some tubules of $TR4^{-/-}$ mice, but quite a few multinucleated giant cells (i.e., SY) can be observed. Sections from at least three $TR4^{+/+}$ and $TR4^{-/-}$ mice at indicated ages were examined, and a representative section is shown. Magnifications: ×1,000 (A, B, C, D, and H); ×400 (E to G). (I and J) DNA flow cytometry analysis of testicular cell suspension obtained from $TR4^{+/+}$ (I) and $TR4^{-/-}$ (J) mice at postnatal day 35. HC, elongated spermatids; 1C, round spermatids; 2C, spermatogonia and nongerm cells; S-ph, spermatogonia synthesizing DNA; 4C, pachytene spermatocytes and G_2 spermatogonia. The arrows indicate the differences between $TR4^{+/+}$ and $TR4^{-/-}$ mice.

tubules have completed meiosis and postmeiosis morphological changes have taken place. Large numbers of round spermatids and elongated spermatids can be seen (Fig. 6E). However, in $TR4^{-/-}$ mice, meiosis is still arrested, germ cell differentiation is still delayed at prophase of meiosis stage, round spermatids still do not appear, and the highest differentiated germ cells are pachytene or diplotene germ cells (Fig. 6F). Eventually, at nearly day 31, germ cells in some tubules of $TR4^{-/-}$ mice testis have completed meiosis and round spermatids appear in these tubules (Fig. 6G and H). However, many SY can be frequently observed (Fig. 6G and H), which could result from spermatocytes with meiosis defects. Furthermore, we determined the frequency distribution histograms of PI-stained testicular cells from $TR4^{+/+}$ and $TR4^{-/-}$ mice at postnatal day 35. As shown in Fig. 6I and J, in $TR4^{-/-}$ mice, the HC cell peak (elongated spermatids) cannot be detected, while the obvious HC cell peak can be detected in $TR4^{+/+}$ mice, indicating the delayed spermatogenesis. The 4C cell peak (most pachytene spermatocytes and few G_1 spermatogonia) was not typical in most $TR4^{-/-}$ mice that we examined in comparison with $TR4^{+/+}$ mice, both at postnatal day 35, suggesting the disruption of spermatogenesis at pachytene spermatocyte stage. Together, the data from Fig. 6 indicated that the late spermatogenesis in $TR4^{-/-}$ mice was caused by delay and disruption at the end of meiotic prophase and subsequent meiotic divisions.

Disrupted tubule-stage characteristics and prolonged and disrupted stage XI to XII in $TR4^{-/-}$ mice. Spermatogenesis is highly organized, with germ cells at particular phases of development joined together into 12 distinct stages in mice. To further confirm the role of TR4 in late prophase and subsequent meiotic divisions, we compared 12 tubule stages between $TR4^{+/+}$ and $TR4^{-/-}$ mice. The characteristics of tubules I to IV are the formation of proacrosomic granules in round spermatids, and we found that there is no difference between $TR4^{+/+}$ and $TR4^{-/-}$ mice in these stages. Figure 7A and B show a typical wild-type stage III tubule and a typical $TR4^{-/-}$ stage III tubule, respectively. The major events of tubule stages V to VIII are the formation of the acrosome cap and testis mature sperm (step 16 spermatids) formed in stage VII, which can be released into lumen in stage VIII. We found that there is no difference between $TR4^{-/-}$ and $TR4^{+/+}$ mice in these stages. Figure 7C and D show a typical wild-type stage VII tubule and a typical $TR4^{-/-}$ stage VII tubule, respectively. The major events of tubule stages IX to XII are the formation of a complete acrosome system in spermatids, the differentiation of late-stage pachytene spermatocytes into diplotene spermatocytes in stage XI, and first and second meiosis shortly taking place in stage XII. We found that there are obvious differences between $TR4^{-/-}$ and $TR4^{+/+}$ mice in stages XI to XII. Meiosis divisions take place quickly in stage XII tubules in $TR4^{+/+}$ mice, and so stages XI to XII in $TR4^{+/+}$ mice were relatively short and only a few metaphase cells were usually observed in the stage XII tubule (Fig. 7E). In contrast, stage XI to XII tubules can be more frequently observed in testes from $TR4^{-/-}$ mice, and in some sections several surrounding tubules are all in stages XI to XII (Fig. 7F). Many different stages of metaphase cells can be observed in seminiferous tubules from $TR4^{-/-}$ mice (Fig. 7F to H). Furthermore, we counted

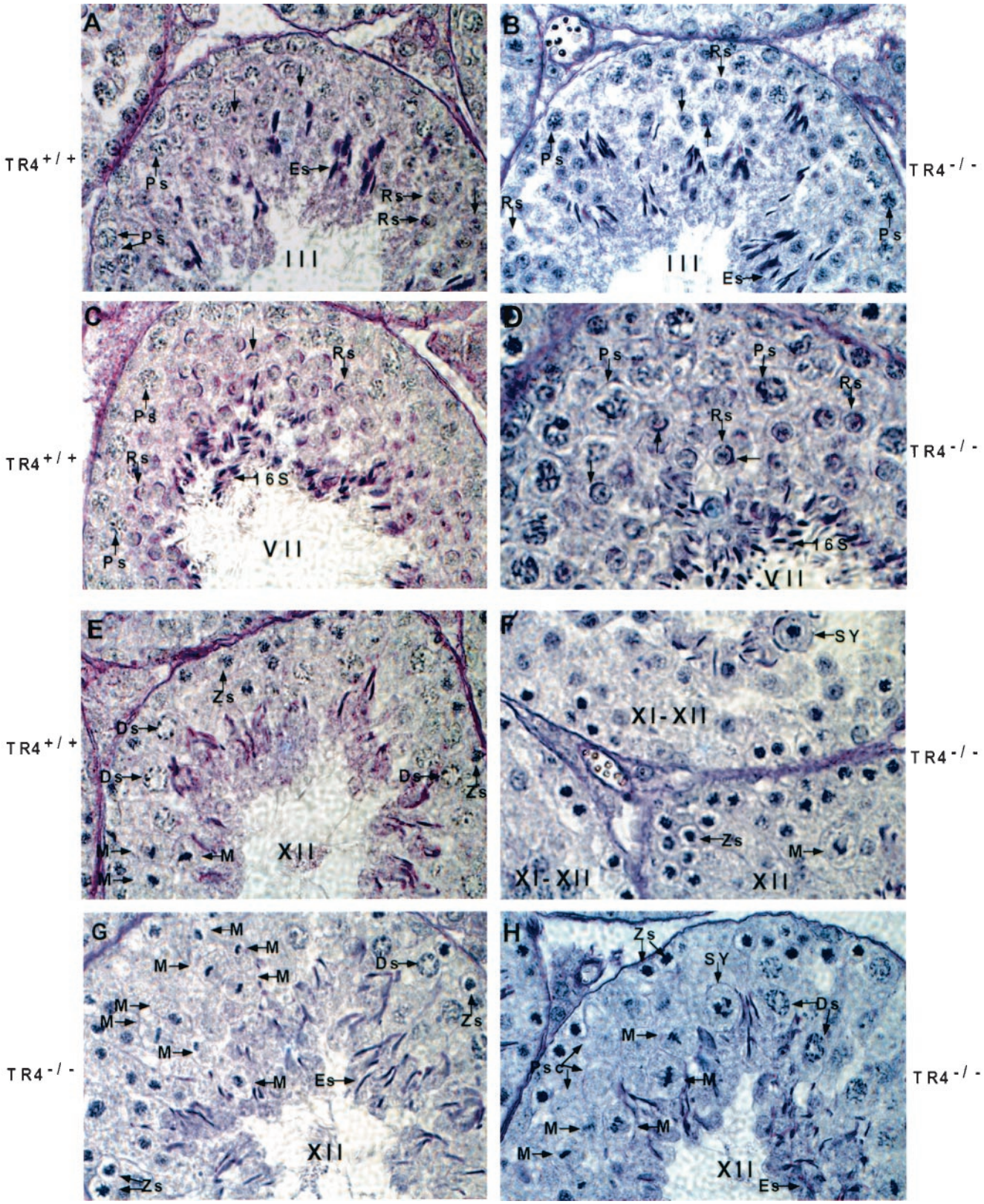

FIG. 7. Disrupted and prolonged tubule stages XI to XII of testes from adult $TR4^{-/-}$ mice. (A) Tubule at stage III from $TR4^{+/+}$ mice. (B) Tubule at stage III from $TR4^{-/-}$ mice. Note the proacrosome granules in round spermatids stained by PAS in both panel A and panel B. (C) Tubule at stage VII from $TR4^{+/+}$ mice. (D) Tubule at stage VII from $TR4^{-/-}$ mice. Note that stage VII tubules from both $TR4^{+/+}$ and $TR4^{-/-}$ mice can produce step 16 testis mature spermatids (16S). No histological difference can be found between panels A and B or panels C and D. (E) Tubule at stage XII from $TR4^{+/+}$ mice. (F to H) Tubules at stages XI to XII from $TR4^{-/-}$ mice. Note prolonged metaphase cells, SY, and

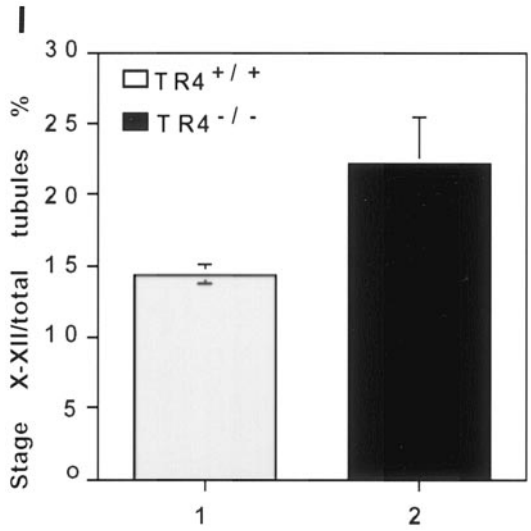

FIG. 7—*Continued*—primary spermatocytes devoid of chromosome structure (Psc). (A to H) Sections from at least three $TR4^{+/+}$ and $TR4^{-/-}$ mice aged 2.5 to 3 months were examined, and a representative section is shown. Magnification, ×1,000. (I) Numbers of stage X to XII tubules and total tubules from each of six testis sections from $TR4^{+/+}$ and $TR4^{-/-}$ mice stained with PAS and hematoxylin were counted, and the ratios of stage X to XII tubules to total tubules were calculated. Results are means ± standard deviations of at least three repeated experiments.

the number of stage X to XII tubules and total tubules from $TR4^{-/-}$ and $TR4^{+/+}$ mice and found that the ratio of stage X to XII tubules is increased in $TR4^{-/-}$ mouse testis (Fig. 7I). Taken together, the results in Fig. 7 clearly indicate that late meiotic prophase and subsequent meiotic divisions are prolonged and disrupted in stage XI to XII tubules in adult $TR4^{-/-}$ mice.

Degeneration and apoptosis in some primary spermatocytes and necrosis in partial seminiferous tubules in $TR4^{-/-}$ mice. Histological examination shows some primary spermatocytes going through degeneration with the appearance of vacuoles in the tubules (Fig. 8A). Necrotic tubules can be found in some of the $TR4^{-/-}$ mice with varying degrees of severity. Figure 8B shows a testis section with severe necrotic seminiferous tubules. As shown in Fig. 8C and D, we also performed a TUNEL assay to assess possible apoptosis. The apoptosis signal can be detected in a few primary spermatocytes in some tubules from $TR4^{-/-}$ mice (Fig. 8C, arrows), but not in tubules from $TR4^{+/+}$ mice (Fig. 8D).

Testis-specific gene expression pattern in $TR4^{-/-}$ mice. To investigate the effect of TR4 deficiency on testis molecular markers and potential downstream targets, we analyzed three panels of testis-specific genes in testis RNA from $TR4^{+/+}$ and $TR4^{-/-}$ mice at different ages (13, 27). One panel of testis-specific genes begins to be transcribed before the first meiotic division, is expressed during the premeiosis phase, and includes the acrosomal serine protease proacrosin (8), the heat

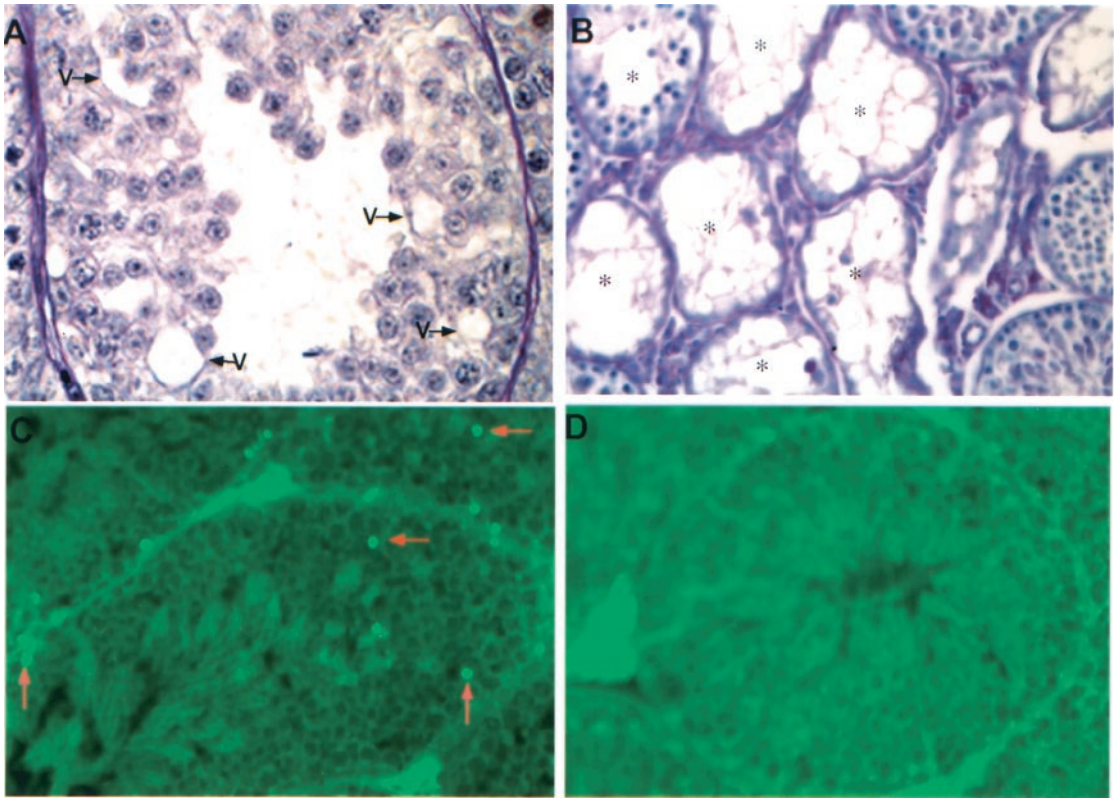

FIG. 8. Degeneration and apoptosis of primary spermatocytes and necrosis of some tubules. (A) Degeneration of primary spermatocytes. V, vacuoles. (B) Necrosis of seminiferous tubules from $TR4^{-/-}$ mice. *, necrotic tubules. (C and D) Detection of apoptosis (arrows) from $TR4^{-/-}$ mice (C) and $TR4^{+/+}$ mice (D). Slides from three $TR4^{-/-}$ or $TR4^{+/+}$ mice were examined, and a representative slide is pictured. Magnification, ×400.

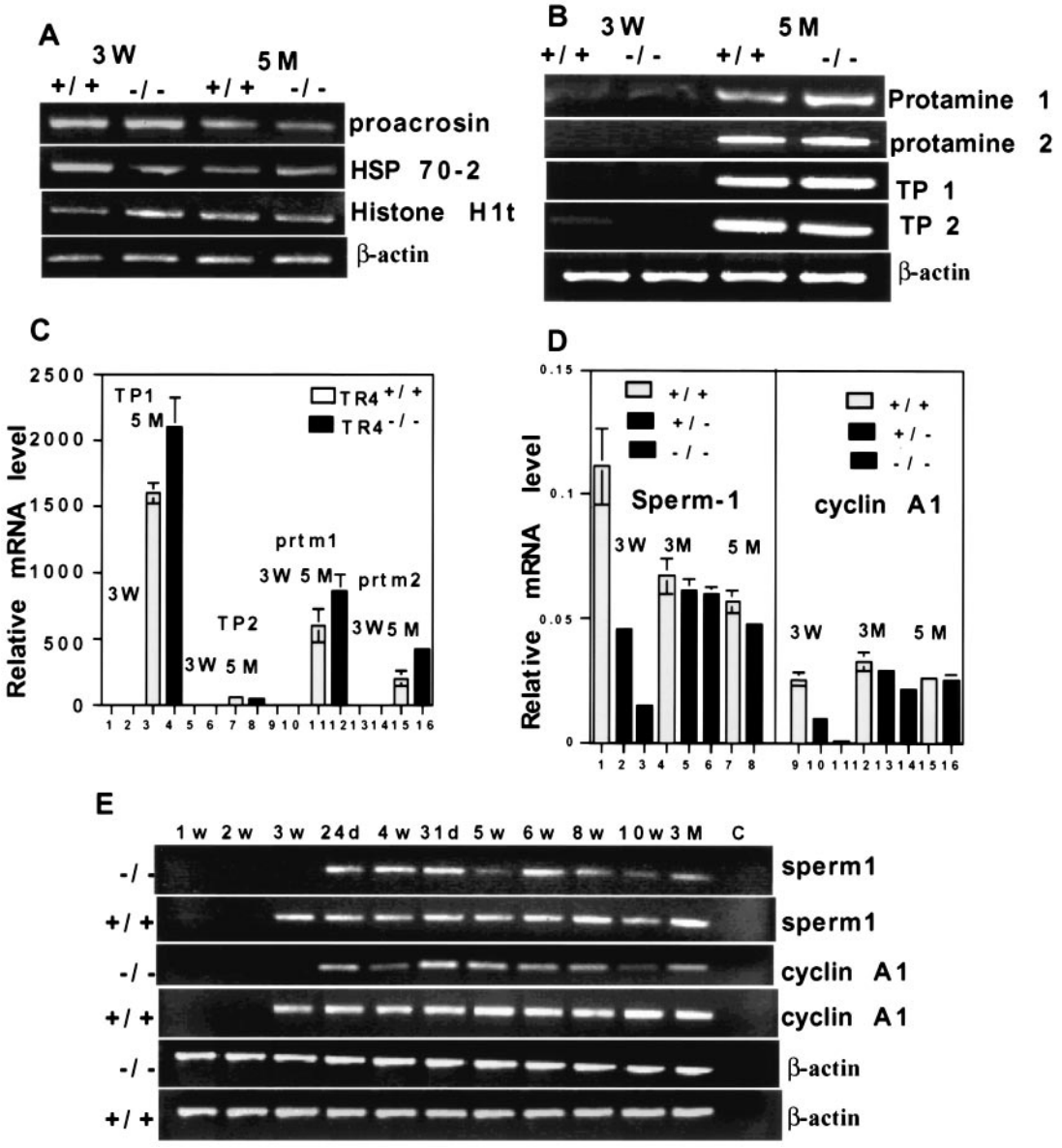

FIG. 9. Analysis of testis-specific gene expression in $TR4^{-/-}$ mice. RT-PCR and real-time quantitative RT-PCR of testis-specific genes were performed. (A) Expression patterns of premeiosis-expressed genes proacrosin, Hsp 70-2, and histone H1t in $TR4^{+/+}$ and $TR4^{-/-}$ mice at indicated ages. W, weeks; M, months. (B) Expression patterns of postmeiosis-expressed genes TP1, TP2, Prm 1, and Prm 2 in $TR4^{+/+}$ and $TR4^{-/-}$ mice at indicated ages. (C) Quantitative analysis of TP1, TP2, prtm1, and prtm2 in $TR4^{+/+}$ and $TR4^{-/-}$ mice at indicated ages. (D) Quantitative analysis of the end of meiotic prophase-expressed genes sperm 1 and cyclin A1 in $TR4^{+/+}$, $TR4^{+/-}$, and $TR4^{-/-}$ mice at indicated ages. (E) Comparison of sperm 1 and cyclin A1 expression patterns between $TR4^{+/+}$ and $TR4^{-/-}$ mice at various developmental and adult stages as indicated by RT-PCR. w, weeks; d, days; C, control. (F) Quantitative analysis of sperm 1 expression pattern in $TR4^{+/+}$ and $TR4^{-/-}$ mice at various developmental and adult stages by real-time RT-PCR. Total RNA was isolated from testes of mice at different ages as indicated in the same manner as for panel E, and real-time quantitative RT-PCR was performed. (G) Quantitative analysis of cyclin A1 expression pattern in $TR4^{+/+}$ and $TR4^{-/-}$ mice at various developmental and adult stages by real-time RT-PCR. Total RNA was isolated from testes of mice at different ages as indicated in the same manner as for panel E, and real-time quantitative RT-PCR was performed. (H) Quantitative analysis of Cyp24a1 expression pattern in adult $TR4^{+/+}$ and $TR4^{-/-}$ mice by real-time RT-PCR. Total RNA was isolated from testes of mice at ages indicated, and real-time quantitative RT-PCR was performed. (A to H) All RT-PCR experiments were repeated three times with RNA samples from two or three different mice. Mouse ages are indicated as postnatal days. β-Actin mRNA was used as internal controls. All real-time RT-PCRs were triplicated and repeated twice with two or three RNA samples from different mice, and all results are normalized with β-actin. All sets of results show the same trend, and one set of data is shown.

shock protein Hsp 70-2 (4, 26), and histone H1t (5). As shown in Fig. 9A, the expression of this panel of genes is not significantly changed in $TR4^{-/-}$ mouse testes compared with that in $TR4^{+/+}$ mouse testes. The second panel of testis-specific genes is expressed during the postmeiotic phase and includes transition protein 1 (TP1), transition protein 2 (TP2), protamine 1 (Prm 1), and protamine 2 (Prm 2) (23). The transitional proteins and protamines are small, highly basic proteins that fa-

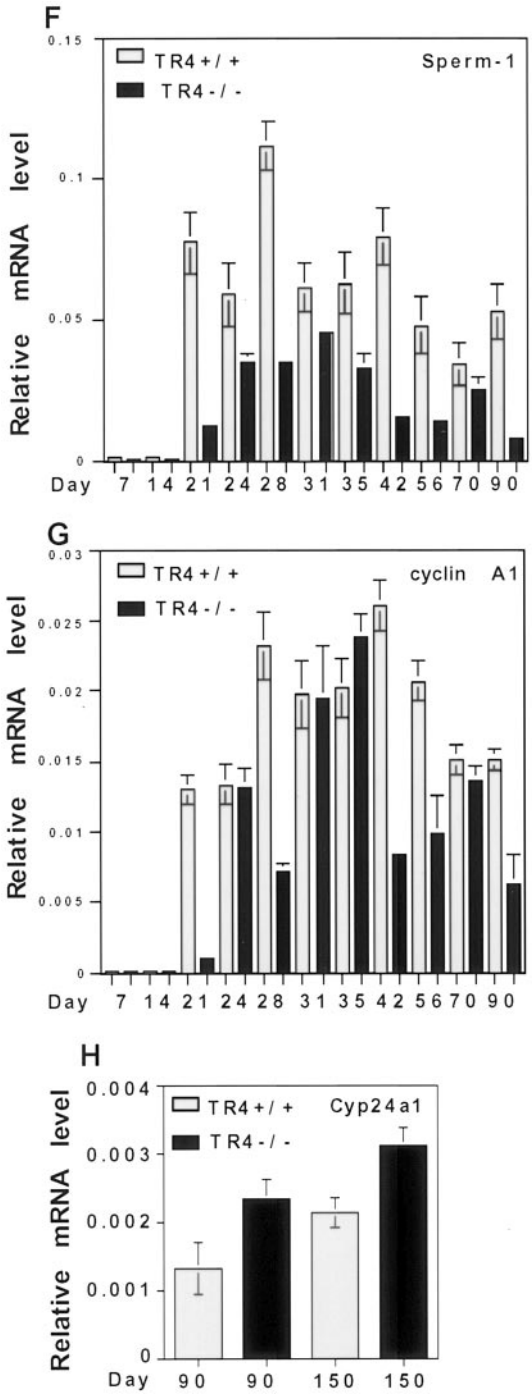

FIG. 9—*Continued*.

cilitate compaction of the mammalian sperm head during spermatogenesis (23). As shown in Fig. 9B and C, the expression of this second panel of genes was not significantly changed or was slightly increased in $TR4^{-/-}$ mouse testes compared to $TR4^{+/+}$ mouse testes. The third panel of genes begins to be expressed at the end of meiotic prophase, plays essential roles in late meiotic prophase and subsequent meiotic division, and includes sperm 1 (1) and cyclin A1 (21). As shown in Fig. 9D, sperm 1 and cyclin A1 are either not detected or only weakly expressed in testes from 3-week-old $TR4^{-/-}$ mice while they are moderately to highly expressed in 3-week-old $TR4^{+/+}$ mouse testes. In adult (5-month) $TR4^{-/-}$ mouse testes, sperm 1 expression level was decreased compared with that in $TR4^{+/+}$ mouse testis, and cyclin A1 expression is also decreased in 3-month-old mice. Furthermore, we detected the expression level of sperm 1 and cyclin A1 at various developmental stages and several adult stages by both RT-PCR and real-time quantitative RT-PCR. As shown in Fig. 9E to G, expression of both sperm 1 and cyclin A1 was delayed in $TR4^{-/-}$ juvenile mice compared with that in $TR4^{+/+}$ juvenile mice. Sperm 1 expression levels in various developmental stages and adult stages were significantly decreased (Fig. 9E and F), and cyclin A1 expression levels in most developmental stages and adult stages were decreased (Fig. 9E and G). Previously, we reported that TR4 could suppress 25-hydroxyvitamin D3, 24-hydroxylase (12), so we also examined the expression level of 25-hydroxyvitamin D3, 24-hydroxylase Cyp24a1 in the testes from adult $TR4^{+/+}$ and $TR4^{-/-}$ mice by quantitative real-time PCR. As shown in Fig. 9H, Cyp24a1 expression increased in the testis from adult $TR4^{-/-}$ mice compared to that from adult $TR4^{+/+}$ mice. This result is consistent with our previous findings.

Figure 10 summarizes the cell types and tubule stages where TR4 and three panels of testis-specific genes are expressed in germ cell progression. In normal testes, TR4 is highly expressed in late-stage primary spermatocytes and early-stage round spermatids in tubule stages IX to XII, and TR4 plays an important role in differentiation of these cells and tubule stages. Knockout of TR4 affects the differentiation and progression of these cells in stages IX to XII, resulting in delayed and disrupted meiotic prophase and subsequent meiotic division and finally sperm production.

DISCUSSION

In this study, we found that TR4 is specifically highly expressed in the primary spermatocytes at meiotic prophase, and TR4 expression dramatically increases and reaches the highest level at this phase during the first wave of spermatogenesis in normal mice. In developing $TR4^{-/-}$ mice, meiotic prophase and subsequent meiotic divisions are significantly delayed and interrupted, resulting in a seriously delayed and disrupted first wave of spermatogenesis. In $TR4^{-/-}$ adult mice, stages XI to XII are prolonged and disrupted, where late meiotic prophase and subsequent meiotic divisions take place, resulting in the increased and prolonged metaphase and appearance of abnormal cells. Delayed and disrupted meiotic prophase and subsequent meiotic divisions can be further confirmed at the molecular level, since the expression of two meiotic prophase-specific genes, sperm 1 and cyclin A1, was delayed at the first wave of spermatogenesis and decreased in most developmental and adult stages in $TR4^{-/-}$ mice. Cyclin A1 has been shown to be a potential new molecular diagnostic marker for male infertility patients (17, 18). Sperm 1-knockout mice show reduced fertility (16). Delayed and decreased expression of sperm 1 and cyclin A1 in $TR4^{-/-}$ mice indicates the role of TR4 in late meiotic prophase and subsequent meiotic divisions. Sperm production in $TR4^{-/-}$ mice is significantly reduced. Together, these data indicate that TR4 plays an important role during late meiotic prophase and subsequent meiotic divisions and

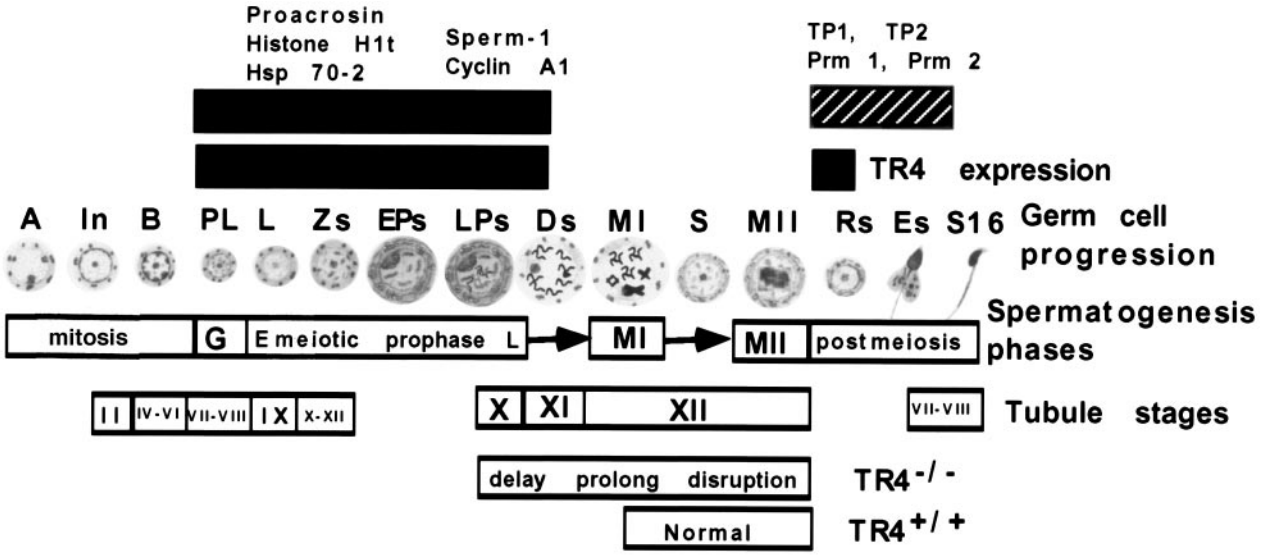

FIG. 10. Diagram of germ cell progression, corresponding to spermatogenesis phase and tubule stages. The black boxes at the top represent the stage showing expression of TR4; end of meiotic prophase-expressed genes sperm 1 and cyclin A1; premeiosis-expressed genes proacrosin, Hsp 70-2, and histone H1t; postmeiosis-expressed genes TP1, TP2, Prm 1, and Prm 2. Note that in TR4$^{-/-}$ mice, late meiotic prophase and subsequent meiotic divisions in late pachytene diplotene and metaphase spermatocytes of tubule stages X to XII were delayed, prolonged, and disrupted. A, type A spermatogonia; In, intermediate spermatogonia; B, type B spermatogonia; PL, preleptotene spermatocytes; L, leptotene spermatocytes; Zs, zygotene spermatocytes; EPs, early pachytene spermatocytes; LPs, late pachytene spermatocytes; Ds, diplotene spermatocytes; MI, first meiosis; MII, second meiosis; Rs, round spermatids; Es, elongated spermatids; S16, step 16 spermatids; E, early; L, late.

that TR4 is essential for normal spermatogenesis. We further analyzed the promoter sequence of cyclin A1, without finding any typical TR4 response elements. The down regulation of cyclin A1 and sperm 1 in TR4$^{-/-}$ mice may be through indirect regulation.

It is known that there are close communication and interaction among testis cell types (20). In TR4$^{-/-}$ mice, the late-stage pachytene spermatocytes and diplotene spermatocytes in some seminiferous tubules could not progress and complete the meiotic divisions, due to disrupted meiotic prophase. This could result in degeneration in other primary spermatocytes in these tubules, which will eventually spread into other testis cells and result in necrosis of these tubules. We observed these necrotic tubules in most testis sections that we examined from TR4$^{-/-}$ mice, which explains why sperm production in TR4$^{-/-}$ mice is significantly decreased.

In juvenile TR4$^{-/-}$ mice, the first wave of spermatogenesis can be finished after several weeks of delay, and in adult TR4$^{-/-}$ mice, although stages XI to XII are prolonged, most tubules can eventually complete meiotic divisions and produce sperm. We believe that some other germ cell-specific genes could compensate for the effect of TR4. We have also examined the expression of TR2, another orphan receptor very closely related to TR4. However, we did not find the increase of TR2 expression in the testes from TR4$^{-/-}$ mice. From previous studies (9, 10, 19, 22), we found that TR4 could be involved in transactivation via protein-protein interactions. The transactivation of these genes may need complicated heterodimer formations, and TR4 and TR2 may be only part of these heterodimer complexes. In the absence of TR4, the other dimerization components might compensate for TR4 effects. Meanwhile, retinoic acid receptor, retinoid X receptor, and many other orphan receptors that share two AGGTCA consensus half-sites with TR4 may also compensate for the TR4 effect.

It is known that many genes play important roles in spermatogenesis. The knockout of some these genes, like AR, could result in arrest of spermatogenesis (13, 24). The knockout of other genes could result in significantly reduced spermatogenesis (16). These latter genes or molecules have a potential to be developed as contraceptive methods. The ligand(s) for TR4 so far is not known, but it is believed that this ligand(s) could be a metabolite with a low molecular weight (9). Further study of the molecular mechanisms through which TR4 plays its essential role in spermatogenesis could help in the development of better medicines for male contraception.

The existence of many infertile human males who exhibit reduced sperm production, but relatively normal mobile spermatozoa, raises the possibility that the reduction of sperm production and fertility of TR4$^{-/-}$ mice would make them potentially useful models for studying subtle events in mammalian reproduction, which may be effective for a subset of the human infertility patients.

ACKNOWLEDGMENTS

This work was supported by the NIH grants DK56984 and DK63212 and the George Whipple Professorship endowment.

The TR4-knockout mice were generated in collaboration with Lexicon Genetics, Inc. We thank Peter Keng of the University of Rochester Cancer Center for assistance in DNA flow cytometry analysis. We also thank Karen Wolf for help in manuscript preparation.

REFERENCES

1. **Anderson, B., R. V. Pearse II, P. N. Schlegel, Z. Cichon, M. B. Schonemann, C. W. Bardin, and M. G. Rosenfeld.** 1993. Sperm 1: a POU-domain gene

transiently expressed immediately before meiosis I in the male germ cells. Proc. Natl. Acad. Sci. USA **90:**11084–11088.
2. **Bellve, A. R., J. C. Cavicchia, C. F. Millette, D. A. O'Brien, Y. M. Bhatnagar, and M. Dym.** 1977. Spermatogenesis cells of the prepuberal mouse. J. Cell Biol. **74:**68–85.
3. **Chang, C., S. F. Da Silva, R. Ideta, Y. F. Lee, S. Y. Yeh, and J. P. H. Burbach.** 1994. Human and rat TR4 orphan receptor specify a subclass of the steroid receptor superfamily. Proc. Natl. Acad. Sci. USA **91:**6040–6044.
4. **Dix, D. J., J. W. Allen, B. W. Collin, P. Poorman-Allen, C. Mori, D. R. Blizard, P. R. Brown, E. H. Goulding, B. D. Strong, and E. M. Eddy.** 1997. HSP70–2 is required for desynapsis of synaponemal complexes during meiotic prophase in juvenile and adult mouse spermatocytes. Development **124:**4595–4605.
5. **Drabent, B., C. Bode, B. Bramlage, and D. Doenecke.** 1996. Expression of the mouse testicular histone gene H1t during spermatogenesis. Histochem. Cell Biol. **106:**247–251.
6. **Hirose, T., W. Fujimoto, T. Yamaai, K. H. Kim, H. Matsuura, and A. M. Jetten.** 1994. TAK1: molecular cloning and characterization of a new member of the nuclear receptor superfamily. Mol. Endocrinol. **8:**1667–1680.
7. **Hirose, T., W. O'Brien, and A. M. Jetten.** 1995. Cloning the gene encoding the murine orphan receptor TAK1 and cell-type-specific expression in testis. Gene **163:**239–242.
8. **Kashiwabara, S., Y. Arai, K. Kodaira, and T. Baba.** 1990. Acrosin biosynthesis in meiotic postmeiotic spermatogenic cells. Biochem. Biophys. Res. Commun. **173:**240–245.
9. **Lee, Y. F., H. J. Lee, and C. Chang.** 2002. Recent advances in the TR2 and TR4 orphan receptor superfamily. J. Steroid Biochem. Mol. Biol. **81:**291–308.
10. **Lee, Y. F., C. R. Shyr, T. H. Thin, W. J. Lin, and C. Chang.** 1999. Convergence of two repressors through heterodimer formation of androgen receptor and testicular orphan receptor-4: a unique signaling pathway in the steroid receptor superfamily. Proc. Natl. Acad. Sci. USA **96:**14724–14729.
11. **Lee, Y. F., W. J. Young, B. P. H. Burbach, and C. Chang.** 1998. Negative feedback control of the retinoid-retinoic acid/retinoid X receptor pathway by the TR4 orphan receptor, a member of the steroid receptor superfamily. J. Biol. Chem. **273:**13437–13443.
12. **Lee, Y. F., W. J. Young, W. J. Lin, C. R. Shyr, and C. Chang.** 1999. Differential regulation of direct repeat 3 vitamin D3 and direct repeat 4 thyroid hormone signaling pathways by the human TR4 orphan receptor. J. Biol. Chem. **274:**16198–16205.
13. **Martianov, L., G. M. Fimia, A. Dierich, M. Parvinen, P. Sassone-Corsi, and I. Davidson.** 2001. Late arrest of spermatogenesis and germ cell apoptosis in mice lacking the TBP-like TLF/TRF2 gene. Mol. Cell **7:**509–515.
14. **Mu, X. M., and C. Chang.** Orphan receptor TR3 mediates apoptosis through up-regulating transcription factor E2F1 in human prostate cancer LNCaP cells. J. Biol. Chem. **278:**42840–42845.
15. **Mu, X. M., Y. X. Liu, L. L. Collins, E. Kim, and C. Chang.** 2000. The p53/retinoblastoma-mediated repression of testicular orphan receptor-2 in the rhesus monkey with cryptorchidism. J. Biol. Chem. **275:**23877–23883.
16. **Pearse, R. V., II, D. W. Drolet, K. A. Kalla, F. Hooshmand, J. R. Bermingham, and M. G. Rosenfeld.** 1997. Reduced fertility in mice deficient for the POU protein sperm-1. Proc. Natl. Acad. Sci. USA **94:**7555–7560.
17. **Schrader, M., C. Muller-Tidow, S. Ravnik, M. Muller, W. Schulze, S. Diederichs, H. Serve, and K. Miller.** 2002. Cyclin A1 and gametogenesis in fertile patients: a potential new molecular diagnostic marker. Hum. Reprod. **17:**2338–2343.
18. **Schrader, M., S. Ravnik, C. Muller-Tidow, M. Muller, B. Staub, S. Diederichs, H. Serve, and K. Miller.** 2002. Quantitation of cyclin A1 and glyceraldehydes 3-phosphate dehydrogenase expression in testicular biopsies of fertile patients by fluorescence real-time RT-PCR. Int. J. Androl. **25:**202–209.
19. **Shyr, C. R., Y. C. Hu, K. Eungseok, and C. Chang.** 2002. Modulation of estrogen receptor-mediated transactivation by orphan receptor TR4 in MCF-7 cells. J. Biol. Chem. **277:**14622–14628.
20. **Skinner, M. K.** 1991. Cell-cell interaction in the testis. Endocr. Rev. **12:**45–77.
21. **Sweeney, C., M. Murphy, S. E. Ravnik, C. F. Hawkins, D. Wolgemuth, and M. Carrington.** 1996. A distinct cyclin A1 is expressed in germ cells in the mouse. Development **122:**53–64.
22. **Tanabe, O., F. Katsuoka, A. D. Campbell, W. M. Song, M. Yamamoto, K. Tanimoto, and J. D. Engel.** 2002. An embryonic/fetal β-type globin gene repressor contains a nuclear receptor TR2/TR4 heterodimer. EMBO J. **21:**1–9.
23. **Wouters-Tytou, D., A. Martinage, P. Chevaillier, and P. Sautiere.** 1998. Nuclear basic proteins in spermatogenesis. Biochimie **80:**117–128.
24. **Yeh, S. Y., M. Y. Tsi, Q. Q. Xu, X. M. Mu, H. Lardy, K. E. Human, S. D. Yeh, S. Altuwaijri, X. C. Zhou, L. P. Xing, B. F. Boyce, M. C. Hung, S. Zhang, L. Gan, and C. Chang.** 2002. Generation and characterization of androgen receptor knockout (ARKO) mice: an in vivo model for the study of androgen receptor function in selective tissues. Proc. Natl. Acad. Sci. USA **99:**13498–13503.
25. **Young, W. J., Y. F. Lee, S. M. Smith, and C. Chang.** 1998. A bi-directional regulation between the TR2/TR4 orphan receptor (TR2/TR4) and ciliary neurotrophic factor (CNTF) signaling pathway. J. Biol. Chem. **273:**20877–20885.
26. **Zakeri, Z. F., D. J. Wolgemuth, and C. R. Hunt.** 1988. Identification and sequence analysis of a new member of the mouse *HSP70* gene family and characterization of its unique cellular and developmental pattern of expression in the male germ line. Mol. Cell. Biol. **8:**2925–2932.
27. **Zhang, D., T. L. Pentila, P. L. Morris, M. Teichmann, and R. C. Roeder.** 2001. Spermatogenesis deficiency in mice lacking the Trf2 gene. Science **292:**1153–1155.